

Avoiding spurious sharpness minimization broadens applicability of SAM

Sidak Pal Singh^{*1}, Hossein Mobahi², Atish Agarwala² and Yann Dauphin²

^{*}Work done during internship at Google DeepMind, ¹ETH Zürich, ²Google DeepMind

Curvature regularization techniques like Sharpness Aware Minimization (SAM) have shown great promise in improving generalization on vision tasks. However, we find that SAM performs poorly in domains like natural language processing (NLP), often degrading performance — even with twice the compute budget. We investigate the discrepancy across domains and find that *in the NLP setting, SAM is dominated by regularization of the logit statistics* — instead of improving the geometry of the function itself. We use this observation to develop an alternative algorithm we call FUNCTIONAL-SAM, which regularizes curvature only through modification of the statistics of the overall function implemented by the neural network, and avoids spurious minimization through logit manipulation. Furthermore, we argue that preconditioning the SAM perturbation also prevents spurious minimization, and when combined with FUNCTIONAL-SAM, it gives further improvements. Our proposed algorithms show improved performance over ADAMW and SAM baselines when trained for an equal number of steps, in both fixed-length and Chinchilla-style training settings, at various model scales (including billion-parameter scale). On the whole, our work highlights the importance of more precise characterizations of sharpness in broadening the applicability of curvature regularization to large language models (LLMs).

Keywords: Sharpness Aware Minimization, Hessian, Generalization, LLMs

1. Introduction

One of the most fundamental questions in machine learning research is: how do we train models that are useful beyond their training data? This question arises in multiple scenarios — from generalizing to unseen samples, dealing with distribution shift, and fine-tuning on specific domains. A commonly held belief is that it is important for models to converge to *well-behaved* and *robust* solutions. The ‘regularity’ of the model is often obtained using *regularization* techniques, which — even in the day and age of LLMs — remain an indispensable part of any training algorithm.

Some of the most prominent regularization methods include weight decay (Krogh and Hertz, 1991), dropout (Srivastava et al., 2014), data augmentation (Ciregan et al., 2012; Krizhevsky et al., 2012), Mixup (Zhang, 2017), and curvature-based controls (Foret et al., 2020; Wu et al., 2020). In recent years, *curvature regularization* techniques have gained popularity due to their effectiveness in promoting

generalization. These techniques bias learning dynamics to areas of lower curvature (i.e., less sharp regions) in the loss landscape (Chaudhari et al., 2017; Foret et al., 2020; Keskar et al., 2017; Pittorino et al., 2020; Wu et al., 2020). The origins of these curvature or *sharpness minimization* techniques can be traced back to the classical ideas of minimum description length (Hinton and Van Camp, 1993; Hochreiter and Schmidhuber, 1997; Rissanen, 1978). Lately, their development has been inspired by their success in a large-scale correlational study (Jiang et al., 2019) and in the NeurIPS generalization competition (Jiang et al., 2020).

Sharpness minimization has demonstrated significant improvement on vision tasks. In contrast, there has not been much uptake of these methods in NLP¹ and, especially for as cornerstone (Brown et al., 2020) a task in NLP as language modeling. Curiously enough, we observe that Sharp-

¹The most notable exception of SAM in NLP is in the fine-tuning scenario (Bahri et al., 2022), where the parameters are constrained to move smaller distances by the very nature of the setup.

ness Aware Minimization (SAM), one of the best studied sharpness regularization methods (Foret et al., 2020), shows poor performance here; indeed, its validation metrics are typically worse than ADAMW throughout training (Figure 1), despite using more computation per step. Hence, this raises the following questions which form the basis of our work:

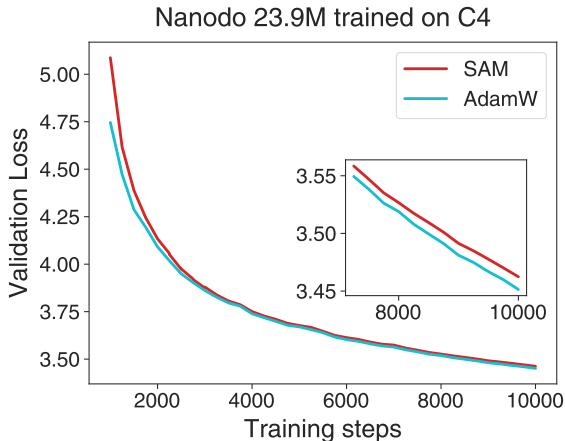


Figure 1 | Evaluation loss curves of ADAMW and SAM for Nanodo decoder-only Transformer model (Liu et al., 2024) on the C4 dataset (Raffel et al., 2020).

What are the reasons for SAM’s poor performance in language modeling? How can they be addressed to successfully yield generalization benefits, while being equal in cost as SAM?

Towards this end, in Section 3, we perform a novel analysis of the path SAM takes to sharpness reduction, and show that it can be split into two contributions — one which modifies the logit statistics to reduce sharpness, and the other which modifies the geometry of the function itself. We measure these two contributions and find that in vision (where SAM works well) the contributions are relatively balanced; in contrast, in language modeling settings the logit path to sharpness minimization dominates.

We hypothesize that the functional path to sharpness minimization needs to be amplified in the language setting, and in Section 4, develop a novel sharpness minimization algorithm called

FUNCTIONAL-SAM that achieves this. Additionally, we motivate another algorithm, PRECONDITIONED SAM, based on preconditioning, and give a theoretical argument that shows it promotes the functional path.

In Section 5, we show that FUNCTIONAL-SAM and PRECONDITIONED SAM provide improvements over baseline ADAMW when trained on the C4 dataset using the Nanodo Transformer codebase (Liu et al., 2024). Moreover, FUNCTIONAL-SAM and PRECONDITIONED SAM can be combined to yield maximal gains. This resulting combination consistently improves validation metrics in both fixed number of steps as well as Chinchilla-like scaling settings (Hoffmann et al., 2022) at a variety of model sizes, spanning three orders of magnitude.

We conclude with an extensive discussion, in Section 7, of additional SAM variants that may be useful in other domains as well as important future directions implied by our work.

2. Setup and Background

Let us assume that we are given data points $\mathbf{z} \in \mathcal{Z}$ drawn i.i.d. from some (unknown) distribution \mathcal{D} , where the samples \mathbf{z} are input-output tuples (\mathbf{x}, \mathbf{y}) , with the input $\mathbf{x} \in \mathbb{R}^d$ of dimension d and the targets $\mathbf{y} \in \mathbb{R}^K$ of dimension K . We seek to model the input-output relation via a neural network $f_{\theta}(\mathbf{x}) : \mathbb{R}^d \mapsto \mathbb{R}^K$ with learnable parameters $\theta \in \mathbb{R}^p$, such that $f_{\theta}(\mathbf{x}) \approx \mathbf{y}, \forall (\mathbf{x}, \mathbf{y}) \in \mathcal{D}$. We take the usual route of empirical risk minimization (Vapnik, 1991) and consider $\theta^* := \operatorname{argmin}_{\theta \in \Theta} \mathcal{L}(\theta)$ with $\mathcal{L}(\theta) := \frac{1}{n} \sum_{i=1}^n \ell(\mathbf{z}_i; \theta)$ and where, $S = \{\mathbf{z}_i\}_{i=1}^n$ is the training set of size n and ℓ denotes the loss function. Hereafter we will consider the loss to be cross-entropy, which is the most popular choice; however, our analyses extend to other loss functions as well.

Under the above setup, Foret et al. (2020) formulates sharpness-aware minimization as the following min-max problem: $\min_{\theta} \max_{\|\epsilon\| \leq \rho} \mathcal{L}(\theta + \epsilon)$, where ϵ denotes a perturbation of the parameters. In particular, the inner maximization is

approximated to first order in the perturbation,

$$\max_{\|\epsilon\| \leq \rho} \mathcal{L}(\theta) + \epsilon^\top \nabla_{\theta} \mathcal{L}(\theta), \quad (1)$$

which subsequently yields $\epsilon^*(\theta) = \rho \nabla_{\theta} \mathcal{L}(\theta) / \|\nabla_{\theta} \mathcal{L}(\theta)\|$ as the optimal perturbation. In SAM (Foret et al., 2020), the authors propose making an update along the direction,

$$\mathbf{g}_{\text{SAM}} = -\nabla_{\theta} \mathcal{L}(\theta + \rho \epsilon^*), \quad \epsilon^* \equiv \frac{\nabla_{\theta} \mathcal{L}(\theta)}{\|\nabla_{\theta} \mathcal{L}(\theta)\|}. \quad (2)$$

3. The Dual Routes to Sharpness Minimization

In this section, we develop a diagnostic tool to understand the failures of SAM in language modeling settings. Our theoretical analysis shows that there are two possible routes to sharpness minimization via SAM—the *logit* path and the *functional* path. We derive quantities which can be used to measure the extent to which each route is active. We find that each path is relatively balanced in vision, but in language modeling settings (where SAM performs poorly) the logit path overwhelms the functional path.

3.1. The Penalty Formalization

We begin by looking at PENALTY-SAM, an alternative version of SAM that is often used in theoretical analyses (Andriushchenko and Flammarion, 2022; Dauphin et al., 2024) and whose gradient matches \mathbf{g}_{SAM} to first order in ρ :

$$\min_{\theta} \mathcal{L}(\theta) + \underbrace{\rho \|\nabla_{\theta} \mathcal{L}(\theta)\|}_{\text{SP}}, \quad (3)$$

We can think of the added gradient norm term as a sharpness penalty SP. To understand how SP influences optimization, we investigate the structure of its gradient:

$$\nabla_{\theta} \text{SP}(\theta) := \rho \frac{\partial}{\partial \theta} \|\nabla_{\theta} \mathcal{L}(\theta)\| = \left(\frac{\partial}{\partial \theta} \nabla_{\theta} \mathcal{L}(\theta) \right) \cdot \epsilon^*(\theta). \quad (4)$$

The gradient itself can be decomposed by the chain rule as

$$\nabla_{\theta} \mathcal{L}(\theta) := \nabla_{\theta} F(\theta) \cdot \nabla_F \mathcal{L}(\theta), \quad (5)$$

where $F(\theta) = (f_{\theta}(\mathbf{x}_1)^\top \cdots f_{\theta}(\mathbf{x}_n)^\top)^\top \in \mathbb{R}^{Kn}$ collates the output over the entire dataset. The first term $\nabla_{\theta} F(\theta)$ represents the Jacobian (derivative of the model function outputs with respect to parameters); while the second term $\nabla_F \mathcal{L}(\theta)$ is the derivative of the loss with respect to the outputs and which comes out to be the difference of the (softmax-ed) logits and the targets.

Using the product rule, we can rewrite Eqn. 4 as,

$$\underbrace{\left[\nabla_{\theta} F(\theta) \cdot \frac{\partial}{\partial \theta} (\nabla_F \mathcal{L}(\theta)) \right]}_{\text{SP gradient from logit perturbation} := \delta_{\text{logit}}} \cdot \epsilon^*(\theta) + \underbrace{\left[\frac{\partial}{\partial \theta} (\nabla_{\theta} F(\theta)) \cdot \nabla_F \mathcal{L}(\theta) \right]}_{\text{SP gradient from perturbing the function Jacobian} := \delta_{\text{func}}} \cdot \epsilon^*(\theta). \quad (6)$$

The first term δ_{logit} represents the *logit-path* to sharpness minimization — directly optimizing the sharpness via the effect of the logits on the loss. In contrast, the second term δ_{func} represents the *functional-path* to sharpness minimization — that is, sharpness minimization via modification of the Jacobian statistics.

3.2. Contribution of Logit and Functional paths

We can explicitly relate the logit and functional paths to sharpness minimization (δ_{logit} and δ_{func} in Eqn. 6) with a decomposition of the Hessian of the loss $\mathbf{H}_{\mathcal{L}} = \nabla_{\theta}^2 \mathcal{L}$,

$$\nabla_{\theta} \text{SP} = \delta_{\text{logit}} + \delta_{\text{func}} = \mathbf{H}_{\text{G}} \cdot \epsilon^* + \mathbf{H}_{\text{F}} \cdot \epsilon^* = \mathbf{H}_{\mathcal{L}} \cdot \epsilon^* \quad (7)$$

where, we use the Gauss-Newton Decomposition of the Hessian (Schraudolph, 2002), namely:

$$\mathbf{H}_{\mathcal{L}} = \mathbf{H}_{\text{G}} + \mathbf{H}_{\text{F}} = \frac{1}{n} \sum_{i=1}^n \nabla_{\theta} f_{\theta}(\mathbf{x}_i) [\nabla_f^2 \ell_i] \nabla_{\theta} f_{\theta}(\mathbf{x}_i)^\top + \frac{1}{n} \sum_{i=1}^n \sum_{k=1}^K [\nabla_f \ell_i]_k \cdot \nabla_{\theta}^2 f_{\theta}^k(\mathbf{x}_i) \quad (8)$$

where, the **Generalized Gauss Newton (GGN)** (\mathbf{H}_{G}) and the **functional Hessian** (\mathbf{H}_{F}) (Singh

et al., 2021, 2023) are the component matrices of the loss Hessian (\mathbf{H}_ℓ). The GGN term captures the curvature of the linearized model; in contrast, the functional Hessian (also known as the Nonlinear Modeling Error (Dauphin et al., 2024)) captures curvature due to model second derivatives.

Thus, we can interpret the *gradient through the logit and functional paths based on the Hessian component they depend upon* — the GGN and functional Hessian respectively.

Normalized composition of Sharpness Gradient. To better gauge which mode of sharpness gradient dominates, we will measure the following natural quantities, τ_{logit} , τ_{func} , τ_{cross} , where the three sum to 1:

$$\begin{aligned}\tau_{\text{logit}} &= \frac{\|\delta_{\text{logit}}\|^2}{\|\nabla_{\theta} \text{SP}\|^2}, \tau_{\text{func}} = \frac{\|\delta_{\text{func}}\|^2}{\|\nabla_{\theta} \text{SP}\|^2}, \\ \tau_{\text{cross}} &= 2 \frac{\langle \delta_{\text{logit}}, \delta_{\text{func}} \rangle}{\|\nabla_{\theta} \text{SP}\|^2}\end{aligned}\quad (9)$$

Hence based on their values, we can realize whether sharpness minimization will prioritise reduction of logit sharpness more or that of functional sharpness, as well as how correlated they are by looking at the cross term.

3.3. Composition of Sharpness Gradient in Practice

We will now analyze SAM’s behavior in language modeling, focusing on how the sharpness gradient composition reveals key differences between its application in language and vision tasks. More concretely, we consider next-token prediction task in the case of language using the C4 dataset and image classification in the case of vision. Since the typical vocabulary sizes in language is in the order of tens of thousands, so besides ImageNet-1K, we adopt other datasets like JFT (Sun et al., 2017) and ImageNet-21K (Ridnik et al., 2021) to make the settings further comparable in terms of number of outputs. For both settings, we employ Transformer-based networks, Nanodo (Liu et al., 2024), which is a simplified version of GPT-2 (Radford et al., 2019), in language modeling and Vision Transformer (ViT, Dosovitskiy et al., 2021) for vision

tasks. Furthermore, in both cases, we train with ADAMW as the optimizer and measure the normalized sharpness gradient contributions (Eqn. 9) throughout training using exact Hessian-vector products. We present the results for Nanodo, C4 as well as ViT with ImageNet-1K and JFT in Figure 2, and that on ImageNet-21K in Appendix A.

Observations. Comparing these figures, we find a stark contrast between the language and vision settings. For vision, we find that the τ_{logit} starts close to 0 but that τ_{logit} and τ_{func} quickly become comparable for most of the training process (Figure 2, top left and top right). In contrast for language, the logit-related gradient fraction τ_{logit} is close to 1 while the sharpness gradient related to the functional part is much smaller Figure 2 (bottom left and bottom right). In all cases, τ_{cross} tends to be negative through most of training (see Figure 4 in the Appendix). This suggests that the two paths to sharpness regularization are antagonistic — taking one path moves you against the other. In language modeling, the dominance of the logit path, combined with negative τ_{cross} , means that the overall contribution from the gradient of SP is unaligned, or even *anti-aligned*, with the functional path to sharpness.

Logit Sharpness vs Functional Sharpness.

The above observations suggest that in NLP settings, SAM is heavily biased towards minimizing sharpness by reducing the gradient of the loss with respect to the logits. There is not much sharpness reduction happening due to making the function more well-behaved. While both of these contribute to decreasing sharpness, the underlying mechanisms show interesting differences. Recalling the relation of logit-sharpness to the Gauss-Newton term \mathbf{H}_G , we see that a simple but spurious way to decrease it is by make the network over-confident about its predictions. This is because of the presence of the term $\nabla_f^2 \ell_i$, which equates to $\text{diag}(\mathbf{p}_i) - \mathbf{p}_i \mathbf{p}_i^\top$, where $\mathbf{p}_i = \text{softmax}(f_\theta(\mathbf{x}_i))$. And thus as \mathbf{p}_i becomes more one-hot (irrespective of leading to the correct output or the incorrect), the logit sharpness will get reduced.

In contrast, the functional sharpness is con-

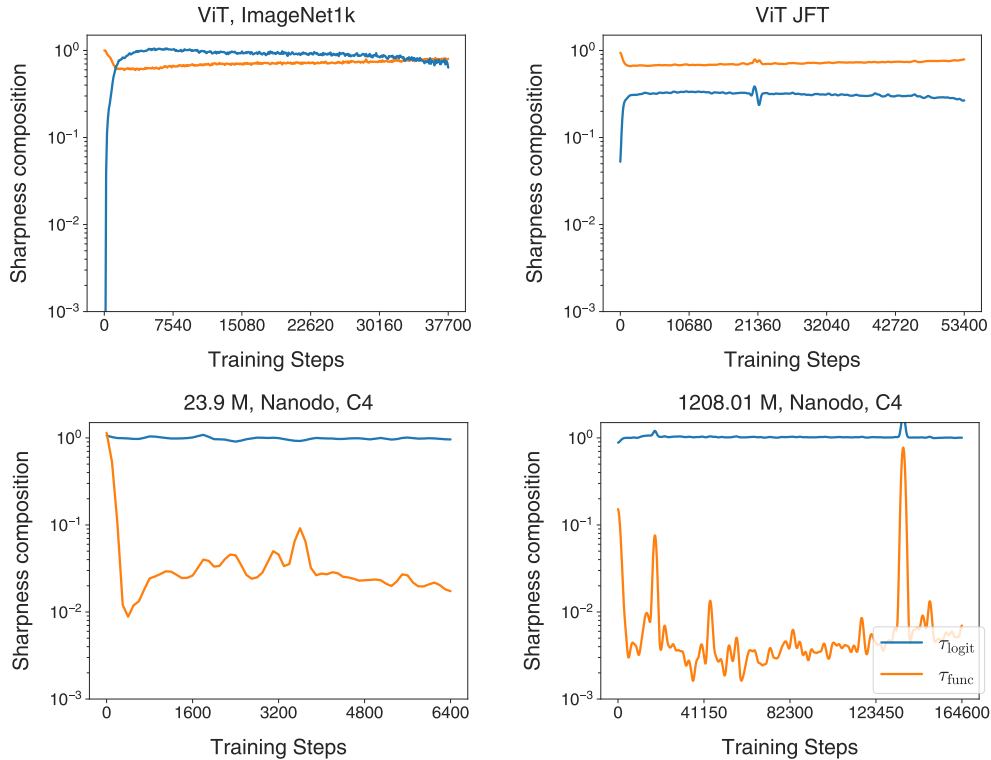


Figure 2 | Normalized sharpness contributions τ_{logit} and τ_{func} show dramatically different trends across modalities. For ViT trained on ImageNet-1K (top left) and JFT (top right), τ_{logit} starts near 0 but quickly increases to a comparable magnitude as τ_{func} . For Transformer models trained on C4 (bottom left and bottom right), $\tau_{\text{logit}} \gg \tau_{\text{func}}$ after the first few steps of training. This suggests that the pathways to sharpness regularization are more imbalanced in NLP compared to vision settings, which may contribute to the poor performance of SAM in NLP settings. τ_{cross} (plotted in Appendix A) is usually negative, suggesting the two methods of sharpness regularization tend to be antagonistic.

nected to the functional Hessian, and the ways of decreasing it (such as via modeling the target better $\mathbf{p}_i \rightarrow \mathbf{y}_i$; or reducing the second-derivative of the function with respect to the parameters $\|\nabla_{\theta}^2 f\| \rightarrow 0$ and hence encouraging a functional simplicity) are intuitively more desirable, even though setting a particular proportion of it might be unclear.

These observations lead to the *hypothesis that if we could encourage a reduction of functional sharpness in lieu of logit sharpness, then sharpness minimization might in fact work for language modeling too*. In the next section, we operate under this hypothesis and derive simple but principled modifications of the SAM update rule.

4. Algorithms to promote the functional path to sharpness minimization

From the PENALTY-SAM formulation in Eqn. 3 and the form of the corresponding sharpness gradients in Eqn. 7, we can see that the functional path to sharpness can, in principle, be amplified by manipulating δ_{logit} and δ_{func} . However, while PENALTY-SAM is competitive with the SAM algorithm, it is less robust than SAM due to ill-behaved second derivatives Dauphin et al. (2024). In contrast to PENALTY-SAM, the perturbation approach in SAM does not explicitly involve second-derivatives in the gradient. Therefore, it is important to develop strategies that promote the functional path using the methodology taken in SAM.

In this section, we discuss two strategies — one direct and the other indirect — that promote the functional path to sharpness minimization, using algorithms which maintain the benefits of the SAM formulation.

4.1. FUNCTIONAL-SAM

The simplest way to promote the functional path would be to use a perturbation which aligns more with δ_{func} than δ_{logit} . We can find such a perturbation by decomposing the SAM update rule from Eqn. 2, as follows:

$$\begin{aligned} \nabla_{\theta} \mathcal{L}(\theta + \rho \epsilon^*) &= \underbrace{[\nabla_{\theta} F(\theta) \cdot \nabla_{\mathcal{F}} \mathcal{L}(\theta + \rho \epsilon^*) - \nabla_{\theta} \mathcal{L}(\theta)]}_{\delta_{\text{logit}} \text{ up to first order in } \rho} \\ &+ \underbrace{[\nabla_{\theta} F(\theta + \rho \epsilon^*) \cdot \nabla_{\mathcal{F}} \mathcal{L}(\theta) - \nabla_{\theta} \mathcal{L}(\theta)]}_{\delta_{\text{func}} \text{ up to first order in } \rho} + \nabla_{\theta} \mathcal{L}(\theta) + O(\rho^2) \end{aligned} \quad (10)$$

The first term is δ_{logit} up to first order in ρ , and the second term is δ_{func} up to first order in ρ . This suggests the following update rule which we call FUNCTIONAL-SAM:

$$\mathbf{g}_{\text{FUNC-SAM}} = -\nabla_{\theta} F(\theta + \rho \epsilon^*) \cdot \nabla_{\mathcal{F}} \mathcal{L}(\theta) \quad (11)$$

where, we discard the δ_{logit} contribution. Further, FUNCTIONAL-SAM uses the same perturbation ϵ^* as the SAM formulation, but *only* perturbs the Jacobian — thus emphasizing the functional path to sharpness as desired. This update rule can be implemented as efficiently as regular SAM using the very same vector-Jacobian product operations that are used to compute gradient in most autodifferentiation frameworks. In Appendix C, we provide the JAX code snippets for SAM and FUNCTIONAL-SAM, demonstrating that the difference in their implementation is a matter of a few lines. Further, like SAM, FUNCTIONAL-SAM remains compatible with methods like ADAMW which take a gradient and then further process it.

Overall, the update rule in Eqn. 11 has the same cost as the SAM update rule, and keeps the benefit of the finite-differences based perturbation approach to sharpness estimation that keeps SAM robust — meeting all our initial goals.

4.2. PRECONDITIONED SAM

In language modeling, Transformers (Vaswani, 2017) are almost exclusively trained with ADAMW or other adaptive methods, and SGD-based training is known to be significantly worse (Liu et al., 2020). This is commonly attributed to the presence of heterogeneity in the gradients (Liu et al., 2020; Noci et al., 2022; Pan and Li, 2023) and the curvature (Jiang et al., 2024; Ormaniec et al., 2024; Zhang et al., 2024) across different “modules” (layer types, layers at different depths, etc.), with the idea that ADAMW alleviates heterogeneity and improves conditioning.

Naively combining SAM and ADAMW creates a potential mismatch — the SAM perturbation is carried out with respect to the unpreconditioned geometry. We hypothesize that this mismatch offers grounds for spurious sharpness minimization. To rectify this, we consider preconditioning the perturbation ϵ^* with the inverse of the same second-moment statistics \mathbf{M} from ADAMW, resulting in the update:

$$\mathbf{g}_{\text{PRECOND SAM}} \equiv -\nabla_{\theta} \mathcal{L} \left(\theta + \rho \mathbf{M}^{-1}(\theta) \epsilon^*(\theta) \right), \quad (12)$$

where $\mathbf{g}_{\text{PRECOND SAM}}$ is then passed to the rest of Adam in lieu of the gradient $\nabla_{\theta} \mathcal{L}(\theta)$.

Another motivation for PRECONDITIONED SAM is that the gradients often align with the principal eigenspaces of $\mathbf{H}_{\mathcal{G}}$ (Gur-Ari et al., 2018). This would amplify δ_{logit} over δ_{func} , since $\delta_{\text{logit}} = \mathbf{H}_{\mathcal{G}} \cdot \epsilon^*$ and ϵ^* is parallel to the gradient. Preconditioning ϵ^* by $\mathbf{H}_{\mathcal{G}}^{-1}$ reduces this effect, thereby *promoting the functional path over the logit path* (see Appendix B.1 for a more detailed argument). Although $\mathbf{H}_{\mathcal{G}}^{-1}$ would be the best preconditioner in this regard, it is expensive to estimate generally and ADAMW already gives us a diagonal estimator in its own preconditioner \mathbf{M}^{-1} at no additional cost.

To conclude, this algorithm (Eqn. 12) has only marginally higher computational cost than standard SAM + ADAMW, and provides an indirect way to improve the contribution of the functional path to sharpness minimization.

5. Empirical Evaluation

5.1. Setup

Training Lengths. In order to evaluate language models of multiple sizes, we consider (pre-)training them in two scenarios: (a) when the training length is kept fixed across scales and (b) when the training length is adjusted as per compute-optimality considerations (Hoffmann et al., 2022; Kaplan et al., 2020).

(a) *Fixed-Length Training Scheme.* In the former, we train all the models for 10K steps, which amounts to seeing roughly a total of 1.3 billion tokens. The results for this setting are presented in Table 2. (b) *Chinchilla-style Training Scheme.* Unlike traditional image-classification based scenarios, training language models often involves determining compute-optimal scaling laws, and whereby models are trained on a corpus size in proportion to their parameters. Specifically, we follow the 20 \times over-training policy suggested in the Chinchilla (Hoffmann et al., 2022) training regime, and use it together with the fixed-depth and globally tuned learning rate scheme, as considered in Everett et al. (2024). The corresponding results are shown in Table 3.

Training Details and Hyperparameters. In either scenario, we consider a batch size of 256 sequences, of maximum length 512, and evaluate model at 5 different sizes: 2M (for prototyping), 23.9M, 42.5M, 117.9M, and 1208M in terms of non-embedding parameters (see details in Appendix A.1), and trained with ADAMW (Kingma and Ba, 2017; Loshchilov and Hutter, 2019) as the underlying optimizer on the C4 dataset (Raffel et al., 2020). We tune the perturbation size ρ separately for each method and model size. The learning rate and weight decay for ADAMW have been tuned across model sizes yielding the values of 0.001, 0.1 respectively. We use the Nanodo (Liu et al., 2024) framework to implement these minimal decoder-only Transformer models, in Flax (Heek et al., 2024) together with JAX (Bradbury et al., 2018).

5.2. Comparison of direct and indirect approaches

Before carrying out an extensive evaluation across different model scales, we do initial prototyping on a smaller model size. This lets us save computational resources and scale up the most promising methods. In particular, we are interested in knowing which methods out of direct and indirect approaches, and their combinations, are most relevant. In Table 1, we present results on a model with 2M non-embedding parameters trained in the fixed-length regime.

Table 1 | *Effect of Preconditioning the SAM perturbation on FUNC-SAM with 2M parameter model.* Lower is better.

METHOD	EVAL LOSS
ADAMW	3.90
SAM	3.91
PRECOND SAM	3.89
FUNC-SAM	3.88
PRECOND FUNC-SAM	3.86

We notice that the plain version of FUNCTIONAL-SAM outperforms both ADAMW and preconditioned SAM. But, FUNCTIONAL-SAM can be further improved by using preconditioning alongside, yielding a significant improvement in terms of evaluation loss. Such second-decimal differences in evaluation loss are typical of the gains provided by new optimization methods for pre-training LLMs look like, e.g., in SOAP (Vyas et al., 2024). Moreover, it should be noted that the standard deviation across different seeds is somewhere in range of the fourth decimal place. Thus, the kind of gains shown in Table 1 are indeed quite significant.

While understanding the exact interplay of preconditioning with FUNCTIONAL-SAM requires further study, the fact that their improvements accumulate suggests that FUNCTIONAL-SAM also benefits from preconditioning through reducing heterogeneity across the modules and alleviating the mismatch between inner and outer optimization geometries in SAM. Hereafter, we will use the preconditioned variant for FUNCTIONAL-

SAM, instead of just the plain FUNCTIONAL-SAM, to reduce the computational costs associated with testing at larger model scales.

5.3. Results at Multiple Model Sizes

Table 2 | Evaluation loss comparison of different methods in a *fixed-length (10K steps) training setup*. Lower is better.

SIZE	PRECOND FUNC-SAM	PRECOND SAM	SAM	ADAMW
23.9 M	3.53	3.55	3.59	3.57
42.5 M	3.41	3.44	3.46	3.45
117.9 M	3.25	3.27	3.29	3.28
1208 M	3.05	NaN	NaN	3.08

Observations. We find that in both the training regimes, our proposed algorithms, namely PRECOND FUNCTIONAL-SAM and PRECOND SAM, significantly outperform SAM as well as ADAMW, at all the model scales in Tables 2 and 3. We find that SAM performs the worst of the lot, even worse than ADAMW while being 2× computationally expensive. Overall, PRECOND FUNCTIONAL-SAM achieves the best results, followed by PRECOND SAM.

At the billion-parameter scale, PRECOND SAM and SAM show susceptibility to numerical instabilities (yielding NaNs) across training regimes, whereas PRECOND FUNCTIONAL-SAM is significantly more robust. In the relatively cheaper fixed-length runs where we could carry out additional investigation, we find that warming up the perturbation radius can mitigate these issues for PRECOND SAM and SAM, yielding an evaluation loss of 3.07 and 3.08, respectively. However, they are still outperformed by our best method, PRECOND FUNCTIONAL-SAM, which obtains a lower evaluation loss of 3.05. and does not need a perturbation warm-up in either training regime.

Also, it should be noted that in the case of larger models, we tune the perturbation radius ρ at a much coarser level to reduce the associated experimental costs. But despite this likely sub-optimal tuning of the ρ for larger models, we

Table 3 | Evaluation loss comparison of different methods in *Chinchilla like training (Everett et al., 2024)*. Lower is better.

SIZE	PRECOND FUNC-SAM	PRECOND SAM	SAM	ADAMW
23.9 M	3.63	3.66	3.71	3.69
42.5 M	3.41	3.43	3.46	3.45
117.9 M	3.10	3.11	3.13	3.12
1208 M	2.61	NaN	NaN	2.63

nevertheless observe consistent gains in performance in both fixed-length and Chinchilla like training regimes.

Discussion. The above-mentioned results demonstrate that the issue with SAM in NLP can be successfully resolved through PRECOND FUNCTIONAL-SAM. The significant improvements in validation performance above are especially intriguing if we bear in mind that these are obtained (a) even when using a *clean corpus such as C4* and (b) training in an *online fashion where no batch is seen more than once* due to massive size of the C4 corpus (even when training for longer duration like in the Chinchilla setup). In industrial training of LLMs, these are idealized conditions which may not always hold and so we can expect further improvements in generalization when training is carried out on noisy corpora and where some parts of it are seen multiple times.

All in all, these results confirm the benefits imparted by FUNCTIONAL-SAM and PRECONDITIONED SAM over SAM, and these improvements in generalization over ADAMW restore the promise of sharpness regularization.

5.4. Ablation Studies

Perturbation strengths. In the above-mentioned results, the best values for SAM typically occur around perturbation radius $\rho = 0.1$, which, in our experiments, happens to be the smallest nonzero perturbation radius considered. However, if we employ larger perturbation radii, the performance of SAM rapidly deteriorates, as shown in Figure 3, which moreover suggests

Table 4 | Comparison of different methods based on Hessian $\mathbf{H}_{\mathcal{L}}$ and GGN \mathbf{H}_G maximum eigenvalue and trace for the 23.9M model trained as per Chinchilla like training setup. Lower is better for all metrics. The best entry is in **bold**, the second best is underlined.

METHOD	EVAL LOSS	$\lambda_{\max}(\mathbf{H}_{\mathcal{L}})$	$\text{tr}(\mathbf{H}_{\mathcal{L}})$	$\text{tr}(\mathbf{H}_G)$
ADAMW	3.69	10.61	4897.52	4745.03
SAM	3.71	2.71	3324.58	3231.46
PRECOND SAM	<u>3.66</u>	<u>5.62</u>	<u>3182.78</u>	<u>3097.87</u>
PRECOND FUNC-SAM	3.63	6.20	2687.12	2503.86

that the optimal value of perturbation size ρ is 0 — i.e., *not using SAM at all*. In contrast, the optimal value of perturbation for PRECOND FUNCTIONAL-SAM tends to be much larger. This explains why we needed to modify the relative magnitudes of the sharpness contributions using PRECOND FUNCTIONAL-SAM—the logit term degrades performance at even small ρ , overwhelming the potential gains from the functional path to sharpness minimization.

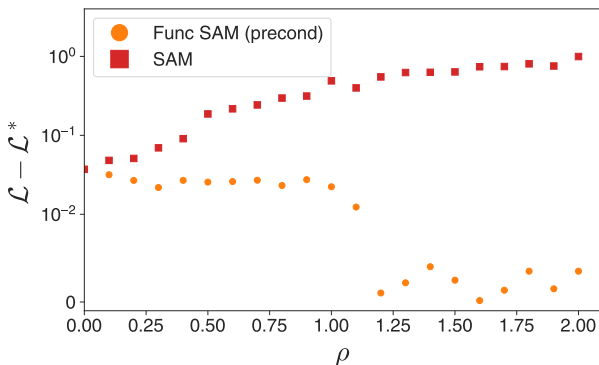


Figure 3 | *Effect of increasing perturbation strengths for SAM and PRECOND FUNCTIONAL-SAM at equal compute.* We see that SAM (red squares) does worse than baseline at non-zero ρ , while PRECOND FUNCTIONAL-SAM (orange circles), with the same compute costs, shows improvements (Nanodo trained on C4, 23.9M parameters, 10K steps). Loss is measured relative to best validation metric for PRECOND FUNCTIONAL-SAM for illustrative purposes.

Non-linearity Choice. While all the above

experimental results utilize GeLU non-linearity, we also carry out experiments with ReLU as the choice of non-linearity. These results can be found in Table 5 of the Appendix, but the key observation is that similar level of improvement is observed in the evaluation loss when using PRECOND FUNCTIONAL-SAM for ReLU based architectures as well.

5.5. Sharpness of Final Solutions

Here, we confirm that the generalization benefits imparted by PRECOND FUNCTIONAL-SAM are brought about convergence to a solution with lower curvature, as shown in the Table 4 for the 23.9M model. Similar results can also be found on other model sizes, and Table 6 of the Appendix shows them for the 117.9M model.

We notice that all sharpness minimization methods yield lower value of the maximum eigenvalue and the trace, as compared to ADAMW. Interestingly, we also that SAM results in the lowest Hessian maximum eigenvalue, even though it performs even worse than ADAMW when evaluating on the validation set. This further highlights how SAM, by default, in language modeling tasks is set up to minimize sharpness spuriously. In contrast, we see that for both of our proposed methods, the improved generalized performance comes hand-in-hand with better landscape properties of their solutions.

6. Related work

Improved variants of SAM in Vision. An extensive line of work has attempted to propose better definitions of sharpness — particularly those which are less sensitive to details of parameterization (Kwon et al., 2021; Li and Giannakis, 2024; Tahmasebi et al., 2024). Some of these methods have shown small improvements on vision tasks. *We believe our decomposition approach is orthogonal to this line of research.* Therefore, the obtained FUNCTIONAL-SAM algorithm is substantially different from prior work.

Studies exploring preconditioning for SAM. Other work has also suggested that the perturbation step in SAM should be taken in an alternative geometry. Our approach to preconditioning is most similar to Fisher SAM (Kim et al., 2022), and the concurrent work of Zhang et al. (2025) which describes a more general preconditioning scheme for SAM. Our key insight is that it is useful to take the SAM perturbation in the *exact same geometry* used by the optimizer, which can be accomplished for negligible cost in the case of Adam and its variants. Furthermore, our work is *primarily driven by the problem of making SAM work in language modeling*, which is far from the focus of these other works.

Role of the indefinite Hessian term. At a more conceptual level, our study aligns with recent works (Dauphin et al., 2024; Singh et al., 2021) which underscore paying more importance to the functional Hessian, the understudied indefinite term of the Hessian in the Gauss-Newton decomposition, as opposed to focusing solely on the positive semi-definite GGN term as suggested by prior studies (Jacot et al., 2020; Pappan, 2019; Sagun et al., 2018). The decomposition of the sharpness gradient into logit and functional modes, along with the demonstrated significance of FUNCTIONAL-SAM in NLP tasks (which is closely tied to the functional Hessian), *highlights the risks of over-reliance on the GGN and the corresponding outlier spectrum of the Hessian* — especially in the context of *regularization of sharpness*.

SAM in NLP. Prior works building on SAM in NLP have been restricted to the fine-tuning set-

ting (Bahri et al., 2022), domain transfer (Sherborne et al., 2024) or on small-scale machine translation setups (Li and Giannakis, 2024). To the best of our knowledge, SAM has hitherto not been successfully applied to language modeling, particularly in any scaling setting.

7. Discussion and Future Work

There are several important aspects that we would like to elaborate on, which could spark interesting future work:

Interpolating smoothly between paths to sharpness minimization. In this work, we focused on FUNCTIONAL-SAM due to our diagnosis of issues in language modeling. However, one can imagine that there might be other domains where FUNCTIONAL-SAM gives spurious minimization, and the alternative “LOGIT-SAM” may need to be emphasized. Our implementation of FUNCTIONAL-SAM can be extended to a more continuous “ANGLE-SAM” which can smoothly interpolate between the extremes, which we discuss in detail in Appendix D. Though we did not find ANGLE-SAM necessary in the language modeling setting, there might be other model-dataset-optimizer triples where it would prove beneficial.

The Perturbation Scope. One of the key takeaways from this work is how scoping the perturbation to the level of the function Jacobian suffices to enable the benefits of SAM in NLP tasks. This scoping can be generalized to *any* set of paths or branches in the computational graph. For example, the output of network with residual connections can be decomposed into multiple streams like $f(\mathbf{x}) = f_1(\mathbf{x}) + f_2(\mathbf{x}) + \dots + f_m(\mathbf{x})$ and practitioners can choose to either have the perturbation go through all or some of them. This perspective opens the door to many more creative levels of perturbation scoping and new regularization techniques.

Optimal Perturbation Transfer. At the largest scales, extensive tuning of the perturbation radius is unfeasible; FUNCTIONAL-SAM and its variants will benefit from improved parameterizations that optimally transfer the

perturbation radius across model scales. The recently explored layerwise perturbation scaling regime for SAM in vision tasks (Haas et al., 2024) may be promising for language too.

Utility for Downstream tasks and deployment. An added advantage of training with sharpness minimization methods is that the resulting flatter solutions can adapt more gracefully to the post-training pipeline, like downstream fine-tuning or model compression. These benefits have been demonstrated in prior work such as (Liu et al., 2023), where a lower Hessian trace at the solution has been shown to correlate better with performance on downstream tasks, and we expect similar benefits to also hold with FUNCTIONAL-SAM and its variants, given the obtained flatter solutions (see Tables 4, 6). Likewise prior work (Na et al., 2022) has also advocated the use of such methods when subsequent model compression is intended, and we also present a very simple demonstration with one-shot pruning in Figure 5 where we see that FUNCTIONAL-SAM shows a more graceful degradation as opposed to ADAMW with increasing sparsity. We leave a detailed study to future work.

Efficiency. A common drawback of sharpness minimization methods is that they require twice the gradient computation per step, and hence are twice as expensive as compared to other optimizers like ADAMW. In this paper, our singular focus has been to address the ineffectiveness of SAM in language modeling, which we have been able to carry out successfully through the proposed FUNCTIONAL-SAM and its preconditioning variants. However, these algorithms still share the same $2\times$ computational burden like SAM itself, and thus additional work is required in the future to make it suitable for deployment. Thankfully, since FUNCTIONAL-SAM is structured similarly to SAM, most advancements in efficient implementations of SAM should be useful for FUNCTIONAL-SAM as well. Given the plethora of recent work in this area for vision (Becker et al., 2024; Du et al., 2022; Liu et al., 2022; Xie et al., 2024), we are optimistic about the development of efficient FUNCTIONAL-SAM variants for language mod-

eling in the near future.

8. Conclusion

Our work thoroughly highlights the ineffectiveness of SAM for language modeling and uncovers the underlying reasons behind such an occurrence. We show that this arises because sharpness reduction in NLP settings is prone to logit manipulation, and hence spurious sharpness minimization, — rather than being driven by promoting the simplicity of the network function. Based on this insight, we propose addressing this issue via FUNCTIONAL-SAM and preconditioning. We demonstrate that both these simple but principled modifications to SAM restore its generalization properties across multiple model scales.

More broadly, we believe that our novel foray into functional and logit modes of sharpness reduction will reinvigorate the existing research into SAM, and pave the way for advanced curvature regularization techniques. Lastly, we are excited about the nuanced characterization of sharpness introduced here and hope that it advances our fundamental understanding of sharpness, its dynamics, and the broader nature of loss landscapes.

References

- M. Andriushchenko and N. Flammarion. Towards understanding sharpness-aware minimization, 2022. URL <https://arxiv.org/abs/2206.06232>.
- D. Bahri, H. Mobahi, and Y. Tay. Sharpness-aware minimization improves language model generalization, 2022. URL <https://arxiv.org/abs/2110.08529>.
- M. Becker, F. Altrock, and B. Risse. Momentum-sam: Sharpness aware minimization without computational overhead, 2024. URL <https://arxiv.org/abs/2401.12033>.
- J. Bradbury, R. Frostig, P. Hawkins, M. J. Johnson, C. Leary, D. Maclaurin, G. Necula, A. Paszke, J. VanderPlas, S. Wanderman-Milne, and Q. Zhang. JAX: composable transformations of Python+NumPy programs, 2018. URL <http://github.com/google/jax>.
- T. B. Brown, B. Mann, N. Ryder, M. Subbiah, J. Kaplan, P. Dhariwal, A. Neelakantan, P. Shyam, G. Sastry, A. Askell, S. Agarwal, A. Herbert-Voss, G. Krueger, T. Henighan, R. Child, A. Ramesh, D. M. Ziegler, J. Wu, C. Winter, C. Hesse, M. Chen, E. Sigler, M. Litwin, S. Gray, B. Chess, J. Clark, C. Berner, S. McCandlish, A. Radford, I. Sutskever, and D. Amodei. Language models are few-shot learners, 2020. URL <https://arxiv.org/abs/2005.14165>.
- P. Chaudhari, A. Choromanska, S. Soatto, Y. LeCun, C. Baldassi, C. Borgs, J. Chayes, L. Sagun, and R. Zecchina. Entropy-sgd: Biasing gradient descent into wide valleys, 2017. URL <https://arxiv.org/abs/1611.01838>.
- D. Ciregan, U. Meier, and J. Schmidhuber. Multicolumn deep neural networks for image classification. In *2012 IEEE conference on computer vision and pattern recognition*, pages 3642–3649. IEEE, 2012.
- Y. N. Dauphin, A. Agarwala, and H. Mobahi. Neglected hessian component explains mysteries in sharpness regularization, 2024.
- A. Dosovitskiy, L. Beyer, A. Kolesnikov, D. Weissenborn, X. Zhai, T. Unterthiner, M. Dehghani, M. Minderer, G. Heigold, S. Gelly, J. Uszkoreit, and N. Houlsby. An image is worth 16x16 words: Transformers for image recognition at scale, 2021. URL <https://arxiv.org/abs/2010.11929>.
- J. Du, D. Zhou, J. Feng, V. Y. Tan, and J. T. Zhou. Sharpness-aware training for free. *arXiv preprint arXiv:2205.14083*, 2022.
- K. Everett, L. Xiao, M. Wortsman, A. A. Alemi, R. Novak, P. J. Liu, I. Gur, J. Sohl-Dickstein, L. P. Kaelbling, J. Lee, et al. Scaling exponents across parameterizations and optimizers. *arXiv preprint arXiv:2407.05872*, 2024.
- P. Foret, A. Kleiner, H. Mobahi, and B. Neyshabur. Sharpness-aware minimization for efficiently improving generalization. *arXiv preprint arXiv:2010.01412*, 2020.
- G. Gur-Ari, D. A. Roberts, and E. Dyer. Gradient descent happens in a tiny subspace. *arXiv preprint arXiv:1812.04754*, 2018.
- M. Haas, J. Xu, V. Cevher, and L. C. Vankadara. μP^2 : Effective sharpness aware minimization requires layerwise perturbation scaling, 2024. URL <https://arxiv.org/abs/2411.00075>.
- J. Heek, A. Levskaya, A. Oliver, M. Ritter, B. Rondepierre, A. Steiner, and M. van Zee. Flax: A neural network library and ecosystem for JAX, 2024. URL <http://github.com/google/flax>.
- G. E. Hinton and D. Van Camp. Keeping the neural networks simple by minimizing the description length of the weights. In *Proceedings of the sixth annual conference on Computational learning theory*, pages 5–13, 1993.
- S. Hochreiter and J. Schmidhuber. Flat minima. *Neural Computation*, 9:1–42, 1997. URL <https://api.semanticscholar.org/CorpusID:733161>.
- J. Hoffmann, S. Borgeaud, A. Mensch, E. Buchatskaya, T. Cai, E. Rutherford, D. de Las Casas, L. A. Hendricks, J. Welbl,

- A. Clark, T. Hennigan, E. Noland, K. Millican, G. van den Driessche, B. Damoc, A. Guy, S. Osindero, K. Simonyan, E. Elsen, J. W. Rae, O. Vinyals, and L. Sifre. Training compute-optimal large language models, 2022. URL <https://arxiv.org/abs/2203.15556>.
- A. Jacot, F. Gabriel, and C. Hongler. The asymptotic spectrum of the hessian of dnn throughout training, 2020. URL <https://arxiv.org/abs/1910.02875>.
- K. Jiang, D. Malik, and Y. Li. How does adaptive optimization impact local neural network geometry? *Advances in Neural Information Processing Systems*, 36, 2024.
- Y. Jiang, B. Neyshabur, H. Mobahi, D. Krishnan, and S. Bengio. Fantastic generalization measures and where to find them, 2019. URL <https://arxiv.org/abs/1912.02178>.
- Y. Jiang, P. Foret, S. Yak, D. M. Roy, H. Mobahi, G. K. Dziugaite, S. Bengio, S. Gunasekar, I. Guyon, and B. Neyshabur. Neurips 2020 competition: Predicting generalization in deep learning, 2020. URL <https://arxiv.org/abs/2012.07976>.
- J. Kaplan, S. McCandlish, T. Henighan, T. B. Brown, B. Chess, R. Child, S. Gray, A. Radford, J. Wu, and D. Amodei. Scaling laws for neural language models, 2020. URL <https://arxiv.org/abs/2001.08361>.
- N. S. Keskar, D. Mudigere, J. Nocedal, M. Smelyanskiy, and P. T. P. Tang. On large-batch training for deep learning: Generalization gap and sharp minima, 2017. URL <https://arxiv.org/abs/1609.04836>.
- M. Kim, D. Li, S. X. Hu, and T. Hospedales. Fisher sam: Information geometry and sharpness aware minimisation. In *International Conference on Machine Learning*, pages 11148–11161. PMLR, 2022.
- D. P. Kingma and J. Ba. Adam: A method for stochastic optimization, 2017. URL <https://arxiv.org/abs/1412.6980>.
- A. Krizhevsky, I. Sutskever, and G. E. Hinton. Imagenet classification with deep convolutional neural networks. *Advances in neural information processing systems*, 25, 2012.
- A. Krogh and J. Hertz. A simple weight decay can improve generalization. *Advances in neural information processing systems*, 4, 1991.
- J. Kwon, J. Kim, H. Park, and I. K. Choi. Asam: Adaptive sharpness-aware minimization for scale-invariant learning of deep neural networks. In *International Conference on Machine Learning*, pages 5905–5914. PMLR, 2021.
- B. Li and G. Giannakis. Enhancing sharpness-aware optimization through variance suppression. *Advances in Neural Information Processing Systems*, 36, 2024.
- H. Liu, S. M. Xie, Z. Li, and T. Ma. Same pre-training loss, better downstream: Implicit bias matters for language models, 2023. URL <https://openreview.net/forum?id=F5uYcwABMu>.
- L. Liu, X. Liu, J. Gao, W. Chen, and J. Han. Understanding the difficulty of training transformers. *arXiv preprint arXiv:2004.08249*, 2020.
- P. J. Liu, R. Novak, J. Lee, M. Wortsman, L. Xiao, K. Everett, A. A. Alemi, M. Kurzeja, P. Marcenac, I. Gur, S. Kornblith, K. Xu, G. Elsayed, I. Fischer, J. Pennington, B. Adlam, and J.-S. Dickstein. Nanodo: A minimal transformer decoder-only language model implementation in JAX., 2024. URL <http://github.com/google-deepmind/nanodo>.
- Y. Liu, S. Mai, X. Chen, C.-J. Hsieh, and Y. You. Towards efficient and scalable sharpness-aware minimization. In *Proceedings of the IEEE/CVF Conference on Computer Vision and Pattern Recognition*, pages 12360–12370, 2022.
- I. Loshchilov and F. Hutter. Decoupled weight decay regularization, 2019. URL <https://arxiv.org/abs/1711.05101>.
- C. Na, S. V. Mehta, and E. Strubell. Train flat, then compress: Sharpness-aware minimization learns more compressible models. In *Findings of the Association for Computational Linguistics: EMNLP 2022*, page 4909–4936. Association for Computational Linguistics, 2022.

- doi: 10.18653/v1/2022.findings-emnlp.361. URL <http://dx.doi.org/10.18653/v1/2022.findings-emnlp.361>.
- L. Noci, S. Anagnostidis, L. Biggio, A. Orvieto, S. P. Singh, and A. Lucchi. Signal propagation in transformers: Theoretical perspectives and the role of rank collapse. *Advances in Neural Information Processing Systems*, 35:27198–27211, 2022.
- W. Ormaniec, F. Dangel, and S. P. Singh. What does it mean to be a transformer? insights from a theoretical hessian analysis, 2024. URL <https://arxiv.org/abs/2410.10986>.
- Y. Pan and Y. Li. Toward understanding why adam converges faster than sgd for transformers. *arXiv preprint arXiv:2306.00204*, 2023.
- V. Pappas. The full spectrum of deepnet Hessians at scale: Dynamics with sgd training and sample size, 2019. URL <https://arxiv.org/abs/1811.07062>.
- J. Pennington and Y. Bahri. Geometry of neural network loss surfaces via random matrix theory. In D. Precup and Y. W. Teh, editors, *Proceedings of the 34th International Conference on Machine Learning*, volume 70 of *Proceedings of Machine Learning Research*, pages 2798–2806. PMLR, 06–11 Aug 2017. URL <https://proceedings.mlr.press/v70/pennington17a.html>.
- F. Pittorino, C. Lucibello, C. Feinauer, E. M. Malatesta, G. Perugini, C. Baldassi, M. Negri, E. Demyanenko, and R. Zecchina. Entropic gradient descent algorithms and wide flat minima. *CoRR*, abs/2006.07897, 2020. URL <https://arxiv.org/abs/2006.07897>.
- A. Radford, J. Wu, R. Child, D. Luan, D. Amodei, I. Sutskever, et al. Language models are unsupervised multitask learners. *OpenAI blog*, 1(8): 9, 2019.
- C. Raffel, N. Shazeer, A. Roberts, K. Lee, S. Narang, M. Matena, Y. Zhou, W. Li, and P. J. Liu. Exploring the limits of transfer learning with a unified text-to-text transformer. *Journal of machine learning research*, 21(140):1–67, 2020.
- T. Ridnik, E. Ben-Baruch, A. Noy, and L. Zelnik-Manor. Imagenet-21k pretraining for the masses, 2021. URL <https://arxiv.org/abs/2104.10972>.
- J. Rissanen. Modeling by shortest data description. *Automatica*, 14(5):465–471, 1978.
- L. Sagun, U. Evci, V. U. Güneş, Y. Dauphin, and L. Bottou. Empirical analysis of the Hessian of over-parametrized neural networks, 2018. URL <https://arxiv.org/abs/1706.04454>.
- N. N. Schraudolph. Fast curvature matrix-vector products for second-order gradient descent. *Neural Computation*, 14:1723–1738, 2002.
- T. Sherborne, N. Saphra, P. Dasigi, and H. Peng. Tram: Bridging trust regions and sharpness aware minimization, 2024. URL <https://arxiv.org/abs/2310.03646>.
- S. P. Singh, G. Bachmann, and T. Hofmann. Analytic insights into structure and rank of neural network Hessian maps. In A. Beygelzimer, Y. Dauphin, P. Liang, and J. W. Vaughan, editors, *Advances in Neural Information Processing Systems*, 2021. URL <https://openreview.net/forum?id=otDgw7LM7Nn>.
- S. P. Singh, T. Hofmann, and B. Schölkopf. The Hessian perspective into the nature of convolutional neural networks. In *Proceedings of the 40th International Conference on Machine Learning*, ICML’23. JMLR.org, 2023.
- N. Srivastava, G. Hinton, A. Krizhevsky, I. Sutskever, and R. Salakhutdinov. Dropout: a simple way to prevent neural networks from overfitting. *The journal of machine learning research*, 15(1):1929–1958, 2014.
- C. Sun, A. Shrivastava, S. Singh, and A. Gupta. Revisiting unreasonable effectiveness of data in deep learning era, 2017. URL <https://arxiv.org/abs/1707.02968>.
- B. Tahmasebi, A. Soleymani, D. Bahri, S. Jegelka, and P. Jaillet. A universal class of sharpness-aware minimization algorithms, 2024. URL <https://arxiv.org/abs/2406.03682>.

- V. Vapnik. Principles of risk minimization for learning theory. *Advances in neural information processing systems*, 4, 1991.
- A. Vaswani. Attention is all you need. *Advances in Neural Information Processing Systems*, 2017.
- N. Vyas, D. Morwani, R. Zhao, I. Shapira, D. Brandfonbrener, L. Janson, and S. Kakade. Soap: Improving and stabilizing shampoo using adam. *arXiv preprint arXiv:2409.11321*, 2024.
- D. Wu, S. tao Xia, and Y. Wang. Adversarial weight perturbation helps robust generalization, 2020. URL <https://arxiv.org/abs/2004.05884>.
- W. Xie, T. Pethick, and V. Cevher. Sampa: Sharpness-aware minimization parallelized, 2024. URL <https://arxiv.org/abs/2410.10683>.
- H. Zhang. mixup: Beyond empirical risk minimization. *arXiv preprint arXiv:1710.09412*, 2017.
- Y. Zhang, C. Chen, T. Ding, Z. Li, R. Sun, and Z.-Q. Luo. Why transformers need adam: A hessian perspective, 2024. URL <https://arxiv.org/abs/2402.16788>.
- Y. Zhang, B. Li, and G. B. Giannakis. Preconditioned sharpness-aware minimization: Unifying analysis and a novel learning algorithm. *arXiv preprint arXiv:2501.06603*, 2025.

Supplementary Materials

A. Additional Results

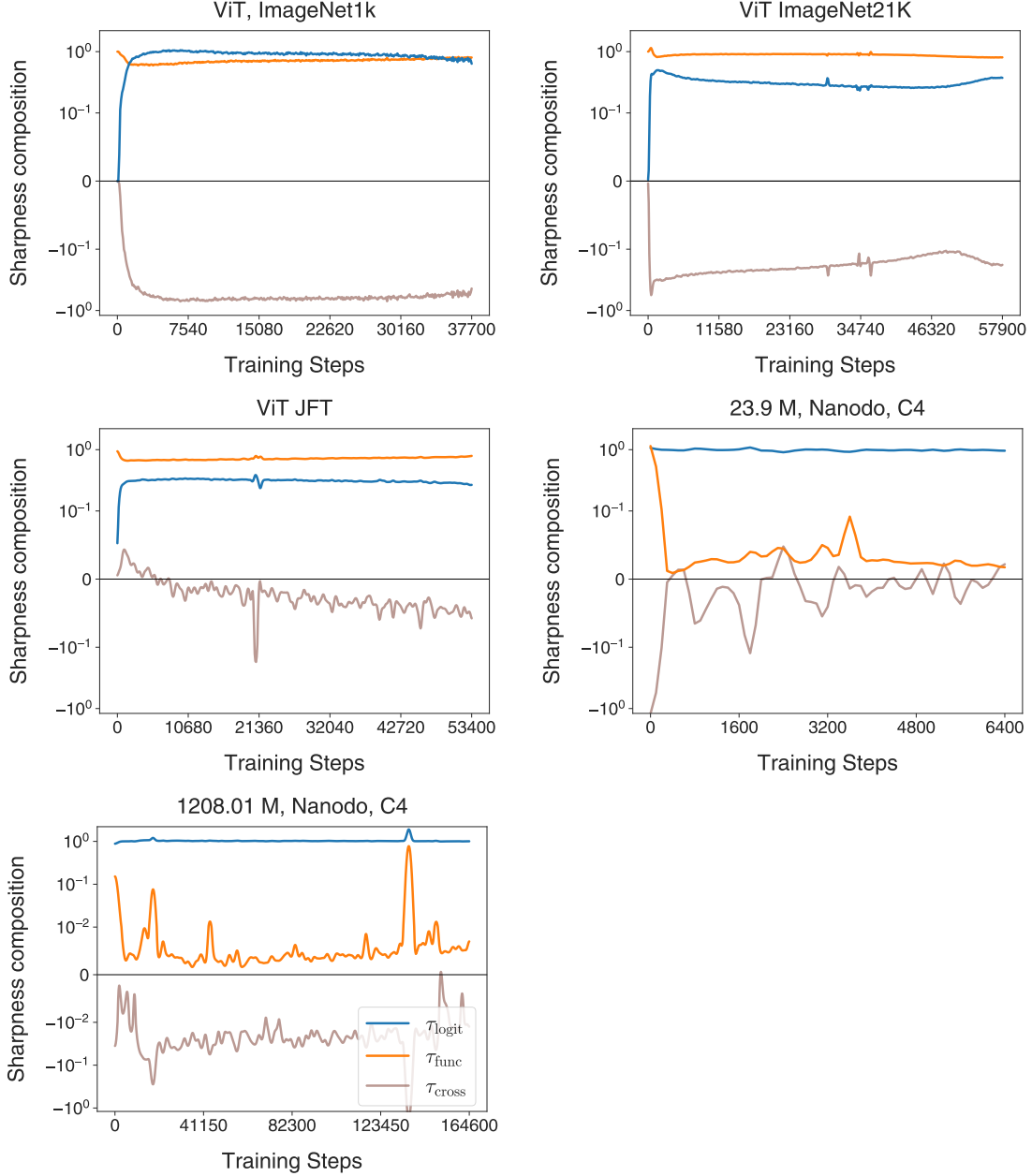


Figure 4 | Sharpness contributions τ_{logit} , τ_{func} and τ_{cross} for various datasets. τ_{cross} tends to be negative for most of training.

A.1. Architectural Details.

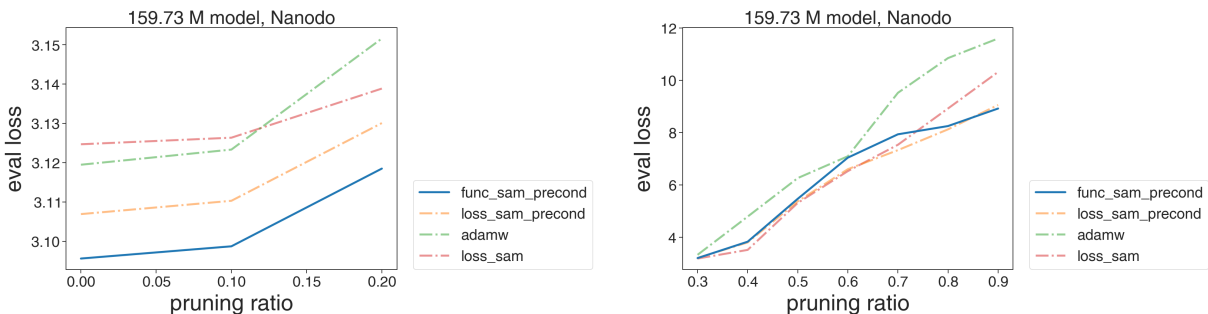
The 23.9M, 42.5M, 117.9M, and 1208M models have the same depth of 6, and whose width has been scaled together with the number of heads. In particular, these correspond to $h = 9, 12, 20,$ and 64 heads per block and the width m scales as $m = 64 \times h$, and the MLP dimension is $f = 4 \times m$. The 2M model used for prototyping has depth 3, 4 heads per block, width $m = 256$ and MLP dimension $f = 1024$.

Table 5 | Comparison of SAM variants across non-linearities for a Nanodo model with 2M (non-embedding parameters) on C4 dataset.

NON-LINEARITY	METHOD	EVAL LOSS
GeLU	PRECOND FUNCTIONAL-SAM	3.8614
GeLU	PRECOND SAM	3.8894
GeLU	ADAMW	3.9069
ReLU	PRECOND FUNCTIONAL-SAM	3.8777
ReLU	PRECOND SAM	3.8937
ReLU	ADAMW	3.9145

 Table 6 | Comparison of different methods based on Hessian $\mathbf{H}_{\mathcal{L}}$ and GGN $\mathbf{H}_{\mathcal{G}}$ metrics for the 117.9M model trained as per Chinchilla like training setup.

METHOD	EVAL LOSS	$\lambda_{\max}(\mathbf{H}_{\mathcal{L}})$	$\text{tr}(\mathbf{H}_{\mathcal{L}})$	$\text{tr}(\mathbf{H}_{\mathcal{G}})$
PRECOND FUNC-SAM	3.096	8.884	2790.650	2746.559
PRECOND SAM	3.108	7.415	2920.445	2060.214
SAM	3.126	3.381	2235.759	2222.779
ADAMW	3.120	9.259	3299.497	3285.881


 Figure 5 | *Effect of one-shot (unstructured) global magnitude pruning*: We see that sharpness minimization methods tend to degrade more gracefully as increasing number of parameters are pruned. Also, from this figure we can see that the performance gained imparted by FUNCTIONAL-SAM over ADAMW is equivalent to setting about 25% parameters of zero, and is thus significant.

B. Additional theory

B.1. Argument for reducing matrix-vector products with inverse preconditioning

We will use a random matrix model to reason about the effects of preconditioning with a matrix inverse. Random matrices have been used to model the spectra of the Hessian of the large models found in machine learning, and in particular treating the Gauss-Newton and the functional Hessian/NME as independent yields quantitative insights about the structure of the overall Hessian (Pennington and Bahri, 2017).

Consider two $N \times N$ symmetric invertible matrices \mathbf{A} and \mathbf{B} . Suppose \mathbf{A} and \mathbf{B} are random and freely independent. Free independence is the non-commutative analog to classical independence, implied by classical independence of entries in the limit of large matrix size (Pennington and Bahri, 2017). The key feature it induces is

$$\mathbb{E}[\text{tr}[\mathbf{A}^j \mathbf{B}^k]] = \mathbb{E}[\text{tr}[\mathbf{A}^j]] \mathbb{E}[\text{tr}[\mathbf{B}^k]] \quad (13)$$

for any j, k , where tr is the trace.

Given a random unit vector \mathbf{v} , the expected squared lengths of the matrix vector products with \mathbf{A} and \mathbf{B} are given by

$$\mathbb{E}[\|\mathbf{A}\mathbf{v}\|^2] = \frac{1}{N} \mathbb{E}[\text{tr}[\mathbf{A}^2]], \quad \mathbb{E}[\|\mathbf{B}\mathbf{v}\|^2] = \frac{1}{N} \mathbb{E}[\text{tr}[\mathbf{B}^2]] \quad (14)$$

The ratio r_1 of magnitudes is given by

$$r_1 \equiv \frac{\mathbb{E}[\|\mathbf{B}\mathbf{v}\|^2]}{\mathbb{E}[\|\mathbf{A}\mathbf{v}\|^2]} = \frac{\mathbb{E}[\text{tr}[\mathbf{B}^2]]}{\mathbb{E}[\text{tr}[\mathbf{A}^2]]} \quad (15)$$

Now consider the norm of $\mathbf{w} = \mathbf{A}^{-1}\mathbf{v}$ passed through each matrix:

$$\mathbb{E}[\|\mathbf{A}\mathbf{w}\|^2] = \frac{1}{N}, \quad \mathbb{E}[\|\mathbf{B}\mathbf{w}\|^2] = \frac{1}{N} \mathbb{E}[\text{tr}[\mathbf{A}^{-1} \mathbf{B}^2 \mathbf{A}^{-1}]] \quad (16)$$

The new ratio of magnitudes r_2 is given by

$$r_2 \equiv \frac{\mathbb{E}[\|\mathbf{B}\mathbf{w}\|^2]}{\mathbb{E}[\|\mathbf{A}\mathbf{w}\|^2]} = \mathbb{E}[\text{tr}[\mathbf{A}^{-1} \mathbf{B}^2 \mathbf{A}^{-1}]] = \frac{\mathbb{E}[\text{tr}[\mathbf{B}^2]]}{\mathbb{E}[\text{tr}[\mathbf{A}^{-2}]]^{-1}} \quad (17)$$

From Jensen's inequality, $\text{tr}[\mathbf{A}^2] \geq \text{tr}[\mathbf{A}^{-2}]^{-1}$. Therefore $r_2 > r_1$; preconditioning by the inverse of \mathbf{A} causes matrix-vector products to upweigh products with \mathbf{B} relative to products with \mathbf{A} , relative to the unpreconditioned product.

In neural network settings, there are non-trivial relationships between the gradient, the Gauss-Newton matrix \mathbf{H}_G and the functional Hessian \mathbf{H}_F ; however, the eigenvectors and eigenvalues of \mathbf{H}_G and \mathbf{H}_F are only weakly related. Therefore even though the exact calculations in the example above don't hold, we suspect that generically preconditioning by \mathbf{H}_G^{-1} will downweigh $\mathbf{H}_G \epsilon^*$ compared to $\mathbf{H}_F \epsilon^*$.

C. Code Snippets for SAM and FUNCTIONAL-SAM

```

from jax import grad, vjp
from jax.tree_util import tree_map
from utils import normalize_grad

def sam_gradients(params, loss_fn, rho):

    # compute the usual loss gradient
    dL_dtheta = grad(loss_fn)(params)

    # normalize the gradients
    dL_dtheta = normalize_grad(dL_dtheta)

    # perturb the parameters
    perturbed_params = tree_map(lambda a, b: a + rho * b, params, dL_dtheta)

    # compute the gradient as by SAM
    sam_grad = grad(loss_fn)(perturbed_params)

    return sam_grad

def functional_sam_gradients(params, loss_fn, network_fn, rho):

    # compute the usual loss gradient, but also extract dL_dlogits
    (dL_dlogits), dL_dtheta = grad(loss_fn, hax_aux=True)(params)

    # normalize the gradients
    dL_dtheta = normalize_grad(dL_dtheta)

    # perturb the parameters
    perturbed_params = tree_map(lambda a, b: a + rho * b, params, dL_dtheta)

    # set up the VJP at the perturbed parameters
    _, dF_dtheta_fn = vjp(lambda theta: network_fn(theta), perturbed_params)

    # do the VJP with the (unperturbed) dL_dlogits
    functional_sam_grad = dF_dtheta_fn(dL_dlogits)[0]

    return functional_sam_grad

```

Listing 1 | Illustration of how to get the gradients in the two methods. Functional SAM differs from the SAM implementation only in the last couple lines, where the effect of perturbation is made to reside only in the function Jacobian part.

D. ANGLE-SAM

In this section, we present a general variant of SAM, which includes both FUNCTIONAL-SAM and SAM as its particular instantiations. The core idea is that once we have been able to decompose the sharpness gradient into those arising from logit and functional paths, we can design our bespoke or custom versions of SAM which lean more or less towards one path than another.

To do so, let's assume that our custom path is at an angle ϕ with the functional path. We weigh the functional path by a factor of $\cos(\phi)$, while we weigh the logit path by $\sin(\phi)$. Then the gradient update in ANGLE-SAM can be described as:

$$\mathbf{g}_{\text{ANGLE-SAM}} := \nabla_{\boldsymbol{\theta}} \mathcal{L}(\boldsymbol{\theta}) + \sin(\phi) \cdot \mathbf{g}_{\text{logit}} + \cos(\phi) \cdot \mathbf{g}_{\text{func}} \quad (18)$$

$$= \nabla_{\boldsymbol{\theta}} \mathcal{L}(\boldsymbol{\theta}) + \sin(\phi) \cdot [\nabla_{\boldsymbol{\theta}} \mathbf{F}(\boldsymbol{\theta}) \cdot \nabla_{\mathbf{F}} \mathcal{L}(\boldsymbol{\theta} + \rho \boldsymbol{\epsilon}^*) - \nabla_{\boldsymbol{\theta}} \mathcal{L}(\boldsymbol{\theta})] + \cos(\phi) \cdot [\nabla_{\boldsymbol{\theta}} \mathbf{F}(\boldsymbol{\theta} + \rho \boldsymbol{\epsilon}^*) \cdot \nabla_{\mathbf{F}} \mathcal{L}(\boldsymbol{\theta}) - \nabla_{\boldsymbol{\theta}} \mathcal{L}(\boldsymbol{\theta})] \quad (19)$$

$$= \nabla_{\boldsymbol{\theta}} \mathcal{L}(\boldsymbol{\theta}) + \rho \sin(\phi) \cdot \mathbf{H}_{\mathbf{G}} \cdot \boldsymbol{\epsilon}^* + \rho \cos(\phi) \cdot \mathbf{H}_{\mathbf{F}} \cdot \boldsymbol{\epsilon}^* + \mathcal{O}(\rho^2) \quad (20)$$

We see that $\phi = \frac{\pi}{4}$ recovers SAM upto first order in ρ , while $\phi = 0$ would yield FUNCTIONAL-SAM and $\phi = \frac{\pi}{2}$ would result in a variant that optimizes solely along the logit path and which can thus be called LOGIT-SAM. *All in all, this shows how ANGLE-SAM is a clean generalization of SAM, that equips it with a perturbation angle in addition to the usual perturbation radius ρ .*

At some level, this above formulation could be viewed as making an assumption that these two paths are orthogonal². On another level, one can simply think of these weights as a mere strategy to obtain convenient weight settings that have their sum of squares as unity.

We expect that this approach might pay dividends in different model-dataset-optimizer triples, and we expect this to be an interesting direction for future work.

²This is not far-fetched. As we noted in our experiments, these two paths tend to be anti-correlated, but often the correlation is quite small in magnitude and approaches zero.